# QUALITY ASSESSMENT OF LIDAR DATA BY USING PAVEMENT MARKINGS

**Charles Toth, Eva Paska**
Center for Mapping
The Ohio State University
Columbus, OH 43212
toth@cfm.ohio-state.edu

**Dorota Brzezinska**
Department of Civil and Environmental Engineering and Geodetic Science
The Ohio State University
Columbus, OH 43210

## ABSTRACT

LiDAR technology has seen remarkable developments in recent years. In particular, the accuracy of the laser ranging has reached the few cm level for hard surfaces, close to static survey performance, and the point density has increased significantly, reaching 150 kHz PRF for multipulse LiDAR systems. These developments allow for better surface representation and exploitation of the 3D nature of the point cloud; in other words, the horizontal accuracy has become an equally important part of the product characterization. The high ranging accuracy of the laser sensor means that overall accuracy of the point cloud is predominantly determined by the quality of the navigation solution (typically based on GPS/IMU sensor integration). Despite recent significant advancements in navigation technologies, to achieve and sustain a high accuracy navigation solution of an airborne platform for longer flight lines over extended time is still a difficult task, as positional drift frequently occur. Moreover, there is no reliable way to assess the positioning quality of the data captured by the laser sensor within the LiDAR system, which is based on direct georeferencing. Therefore, using some ground control is almost mandatory if high accuracy is required. This paper introduces a method to use road pavement marking as ground control that could be used for QA/QC. These linear features are widely available in urban areas and along transportation corridors, where most of the government and commercial mapping takes place.

## INTRODUCTION

Since its introduction in the late 90s, LiDAR has seen remarkable developments, mainly driven by technology. For the user, it means higher point density, or better surface representation, and improving accuracy. The state-of-the-art is that the laser sensor can provide 1-2 cm ranging accuracy for so-called hard surfaces at normal flying heights; which means that the georeferencing term accounts primarily for the accuracy of the LiDAR product. Despite consistent advancement of the GPS/IMU-based georeferencing technology for longer flight lines, the performance of the navigation solution could change, resulting in a varying accuracy of the LiDAR point cloud. The main effect is that strip overlap areas could show varying amount of discrepancies; typically, described as drift. While a strip adjustment can eliminate the strip differences, the absolute accuracy is not necessarily improved as a result of the applied correction. Therefore, ground control is always needed as there is no other way to independently validate the accuracy of the LiDAR product, including both the vertical and horizontal terms. The methodology to characterize a LiDAR product using ground control includes several components, such as the determination of the differences between LiDAR data and reference surfaces, requirement for the number of ground control areas, analysis of the distribution of the differences, statistical method used, specification and qualification of the results, etc. This paper is only addressing the measurements of discrepancies.

The evolution of ground control used for product QA/QC is closely related to the improvements in the LiDAR point density. When sparsely distributed points were available, the vertical accuracy was the only concern (ASPRS Guidelines, 2004). In fact, the horizontal characterization was greatly ignored at the introduction of LiDAR technology. Obviously, from a theoretical point of view, points separated by a few meters did not allow for adequate surface characterization in general, except for flat areas. To assess the vertical accuracy of the point cloud, flat horizontal surfaces with precisely known elevation can be used. Once the vertical difference was measured, usually based on the statistics derived from a sufficient number of points over flat surface patchs, either a simple vertical shift was applied as correction or a more complex model could be used that factored in surface differences observed at several (well distributed) locations.

As density increased, however, the need for characterizing the point cloud in 3D terms became important, which ultimately required the measurements of 3D surface discrepancies. Methods were soon developed to determine surface discrepancies that could be applied to both LiDAR strips and reference surfaces. Obviously, 3D observations are only available if there is sufficient terrain relief, in which case the problem is solved by surface matching (e.g., Besl and McKay, 1992; Gruen and Akca, 2005). There is a variety of methods that can handle any kind of surfaces or can use a number of planar surface patches with different surface normal vectors. A practical aspect of the surface matching is that it is rather difficult to precisely survey ground surfaces of any shape in general, although terrestrial laser scanning is becoming a viable solution for this purpose. Using man-made objects, such as buildings, provides an easier approach to develop a reference test range with many differently oriented planar surfaces. In fact, airport areas are frequently used for laser sensor calibration.

The use of dedicated LiDAR targets is another alternative to observe LiDAR point cloud differences at reference points and, consequently, to estimate errors. One of the first approaches to use LiDAR-specific ground targets was developed at OSU (Csanyi and Toth, 2007). The circular-shaped targets, optimized for a point density of 3-4 pts/$m^2$ and above, had a diameter of 2 m and used a different reflective coating on the center circle and outer ring. At the required point cloud density, the number of points returned from the targets allowed for accurate estimation of both vertical and horizontal differences. The technique has been used in several projects and provided highly accurate ground control for QA/QC (Toth *et al*., 2007a). In a similar implementation, small retro reflectors are placed in a certain shape of similar size, in which case the construction of the target is simpler while the processing is more complicated. Although, these solutions provide excellent results, their use is somewhat limited by economic factors; i.e., the installation and the necessary survey of the targets could be quite labor-intensive. Note that the processing of the LiDAR-specific ground targets is highly automated, and human intervention is only needed for the final evaluation of the results.

To advance the use of ground targets for transportation corridor surveys, an economic method is proposed here that can achieve comparable results using LiDAR-specific ground targets (Toth *et al*., 2007b). The use of pavement markings as ground control offers the advantage of being widely available in excellent spatial distribution, and requires no installation. Certainly, the surveying of the targets is still needed, but it becomes less difficult with the increasing use of GPS VRS systems that can provide cm-level accuracy in real-time. The other condition of using pavement markings is the availability of LiDAR intensity data that is hardly a restriction with modern LiDAR systems. Note that the distinct appearance of the pavement markings in the LiDAR intensity image is essential for the proposed method, see Figure 1. The main steps of using pavement marking as ground control are briefly described in this paper.

(a) (b)

**Figure 1.** Pavement marking appearance in LiDAR intensity image (a) and reference optical image (b).

## USING PAVEMENT MARKINGS AS GROUND CONTROL

The concept of the proposed method, including pavement marking extraction together with the parameterization of the marks based on LiDAR intensity data, the comparison with ground truth, and the determination of a transformation to correct the point cloud, analysis of result, etc., is shown in Figure 2. The GPS-surveyed data of the pavement markings, represented in a series of points with cm-level accuracy is assumed to be available. For sensor calibration and/or strip adjustment, sufficient number of pavement markings with good spatial distribution is required to achieve good performance. Currently, only the most widely found types of pavement markings are considered: Stop bars, straight edge lines and curved edge lines. In each case, the survey data of the pavement markings is provided as point observations along the centerline of the markings. The LiDAR data, including range and intensity components, are assumed to be of reasonable quality; i.e., no gross errors and thus the point cloud accuracy is better than a meter.

Based on the comparison of the two descriptions of pavement markings, one obtained from the GPS survey and the other one form LiDAR intensity and range data, 2D/3D offset and orientation differences can be detected. Since the road surfaces are predominantly flat and mostly horizontal, the horizontal and vertical discrepancies can be separated in most of the cases. Analyzing the magnitude of the observed differences and their spatial distribution, the LiDAR data quality can be assessed and, if needed, corrections can be applied to the LiDAR point cloud to improve the point position accuracy. The methodology for the correction could be based on either introducing a spatial transformation to reduce the differences at the controls or trying to adjust the sensor parameters to achieve the same objective. In most of the cases, a 3D similarity transformation is applied and the accuracy terms for both data sets are needed to properly characterize the data quality after applying the correction. Note that assessing the horizontal accuracy of the LiDAR point cloud is difficult, as it is mainly defined by the footprint of the laser pulse, which depends on flying height and beam convergence; in addition, the impact of object surface characteristics could be also significant. In the following, the three key components of the proposed method, pavement marking extraction, curve fitting and matching are discussed at detail.

### Extraction of Pavement Markings

The extraction of the pavement markings is based on the significant difference in the LiDAR intensity values between road surfaces and pavement markings. Furthermore, the availability of GPS survey data of the pavement markings drastically reduces the search window for the extraction process (the selection of LiDAR points obtained from the pavement markings). Depending on the overall LiDAR data quality, more precisely the horizontal accuracy of the point cloud, the actual search area is typically a narrow patch with a width of less than 1 m. Unfortunately, the relative nature of the LiDAR intensity signal does not allow for a general parameterization of the intensity values for pavement surfaces and pavement markings. Therefore, first the distribution of the intensity signals in the search window should be analyzed to determine an optimal threshold for separating pavement and pavement marking points. The points extraction based on the threshold could result in errors such as marking points are omitted or pavement points are included. Therefore, further checks are needed, which is accomplished by curve fitting, described below, where the availability of object space information can be utilized, such as curvature of the pavement markings. To illustrate the difficulty of the extraction process, Figure 3 shows the troubling case when the LiDAR scan line is near parallel to the pavement marking.

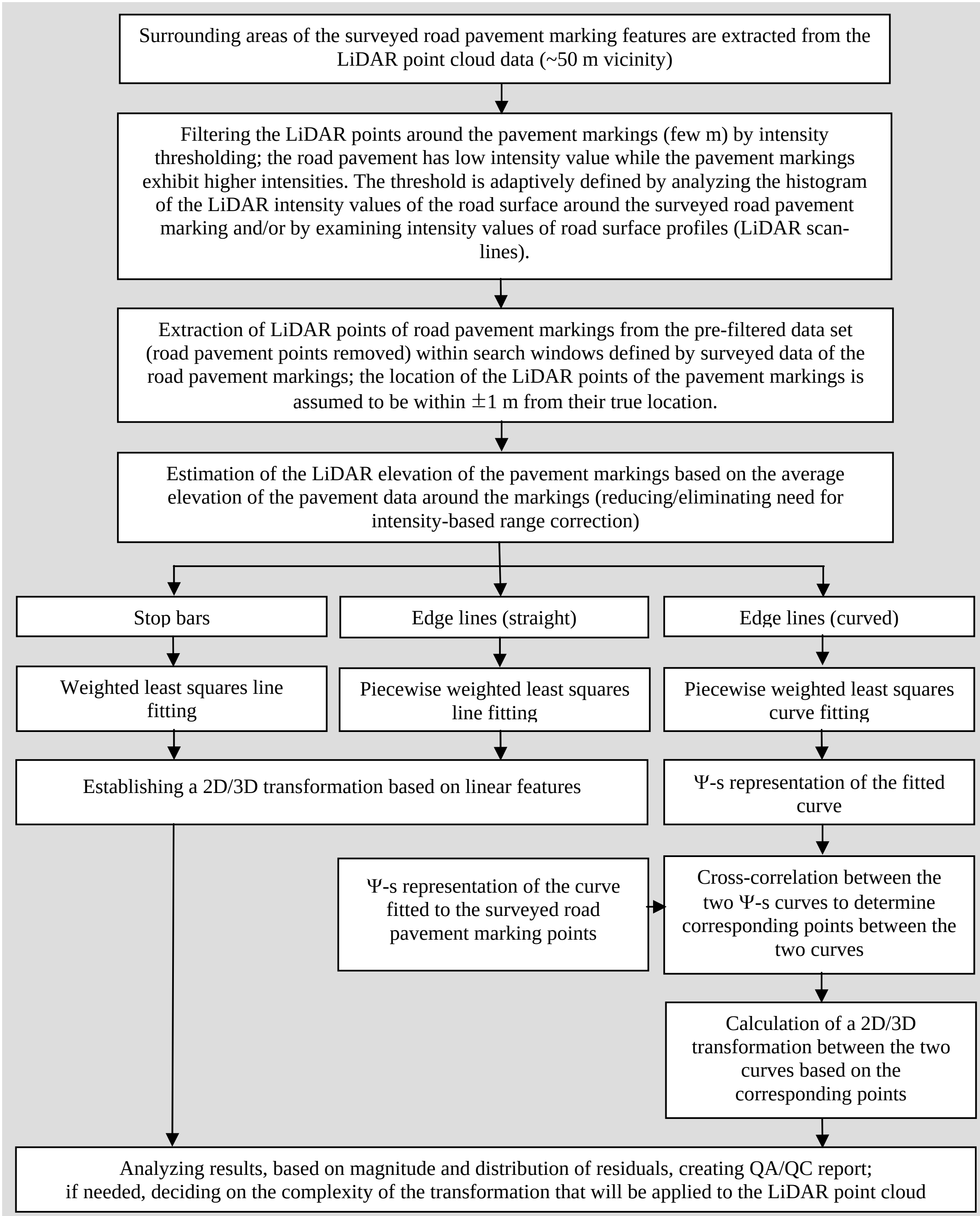


**Figure 2**. Concept of extracting pavement markings and using them as ground control.

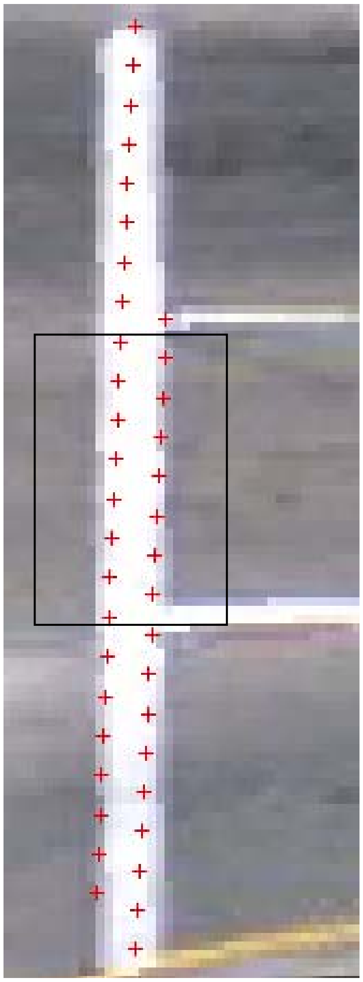

(a)

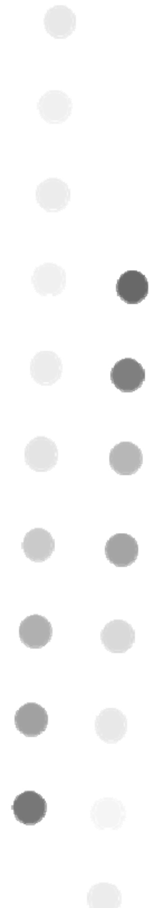

(b)

**Figure 3.** Changes of intensity values along pavement markings: LiDAR point locations overlaid on optical image (a) and intensity values (b).

## Curve Fitting

The purpose of curve fitting is twofold: first, it provides a validity check for the pavement marking points extracted, and second, it allows for modeling both pavement marking descriptions as linear features, so they can be matched to each other. The selected curve fitting method is an extended version of the algorithm, originally proposed by Ichida and Kiyono in 1977, and is a piecewise weighted least squares curve fitting based on cubic (third-order polynomial) model, which seemed to be adequate for our conditions, linear features with modest curving. To handle any kind of curves, defined as the locus of points f(x, y) = 0 where f(x, y) is a polynomial, the curve fitting is performed for smaller segments in local coordinate systems, which are defined by the end points of the curve segments. The primary advantage of using a local coordinate system is to avoid problems when curves become vertical in the mapping coordinate system. Obviously, the fitting results as well as the fitting constraints are always converted forth and back between the local and mapping coordinate frames.

The main steps of the piecewise cubic fitting (PCF) process are shortly discussed below; the notation used in the discussion is introduced in Figure 4. To achieve a smooth curve, the curve fitting to any segment is constrained by its neighbors by enforcing an identical curvature at the segment connection points; in other words, PCF polynomial is continuous with its first derivative at connection points $x=s$, $x=t$, etc. The equations describing the third-order polynomial and its first derivative are:

$$S_k(x) = y_s + m_s \cdot (x-s) + a_s \cdot (x-s)^2 + b_s \cdot (x-s)^3$$

$$\text{slope} = S_k{}'(x) = m_s + 2 \cdot a_s \cdot (x-s) + 3 \cdot b_s \cdot (x-s)^2$$

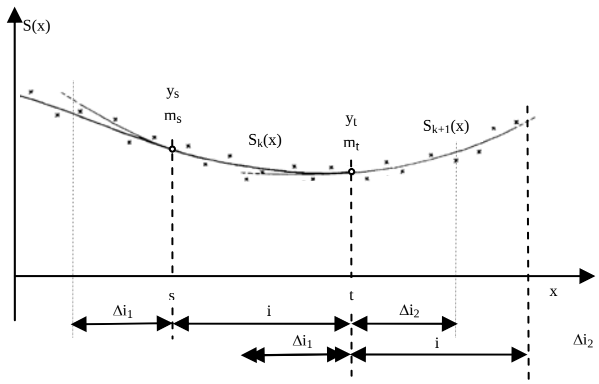


**Figure 4**. Piecewise weighted least squares curve fitting method.

The core processing includes the following steps: 1) $a_S$ and $b_S$, the coefficients of the second and third order terms of the fitted curve for interval '*i*' are estimated; consider the constant term ($y_S$) and the coefficient of the first order term ($m_S$) fixed, known from the curve fitting from the previous segment. In the adjustment, the points in interval $\Delta\ i_2+\ i+\Delta\ i_1$ (past, present, and future data points) are used, 2) the value ($y_t$) and the slope ($m_t$) at $x=t$ are computed; these values as fixed constraints are used in the curve fitting for the next segment, and 3) step 1 is repeated to process the next segment.

| | |
|---|---|
| Step 1 | $y - y_s - m_s \cdot (x-s) = a_s \cdot (x-s)^2 + b_s \cdot (x-s)^3$<br>LS for points in interval $\Delta \mathrm{i}_1 + i + \Delta \mathrm{i}_2 \Rightarrow \hat{a}_s, \hat{b}_s$<br>$\Rightarrow S_k(x) = y_s + m_s \cdot (x-s) + \hat{a}_s \cdot (x-s)^2 + \hat{b}_s \cdot (x-s)^3$ |
| Step 2 | $\rightarrow x = t$<br>$\hat{y}_t = S_k(t) = y_s + m_s \cdot (t-s) + \hat{a}_s \cdot (t-s)^2 + \hat{b}_s \cdot (t-s)^3$<br>$\hat{m}_t = S_k'(t) = m_s + 2 \cdot \hat{a}_s \cdot (x-s) + 3 \cdot \hat{b}_s \cdot (x-s)^2$<br>$\rightarrow y_t = \hat{y}_t \ \ and \ \ m_t = \hat{m}_t$ |
| Step 3 | $S_{k+1}(x) - y_t - m_t \cdot (x-t) = a_t \cdot (x-t)^2 + b_t \cdot (x-t)^3$<br>LS for points in interval $\Delta \mathrm{i}_1 + i + \Delta \mathrm{i}_2 \Rightarrow \hat{a}_t, \hat{b}_t$ |

The curve fitting allows for a polyline representation of both data types, LiDAR or GPS, with a user-defined spacing and thus can effectively curve fitting. Figure 5 shows curve fitted to LiDAR points as well as a case where both data data sets were modeled by curves.

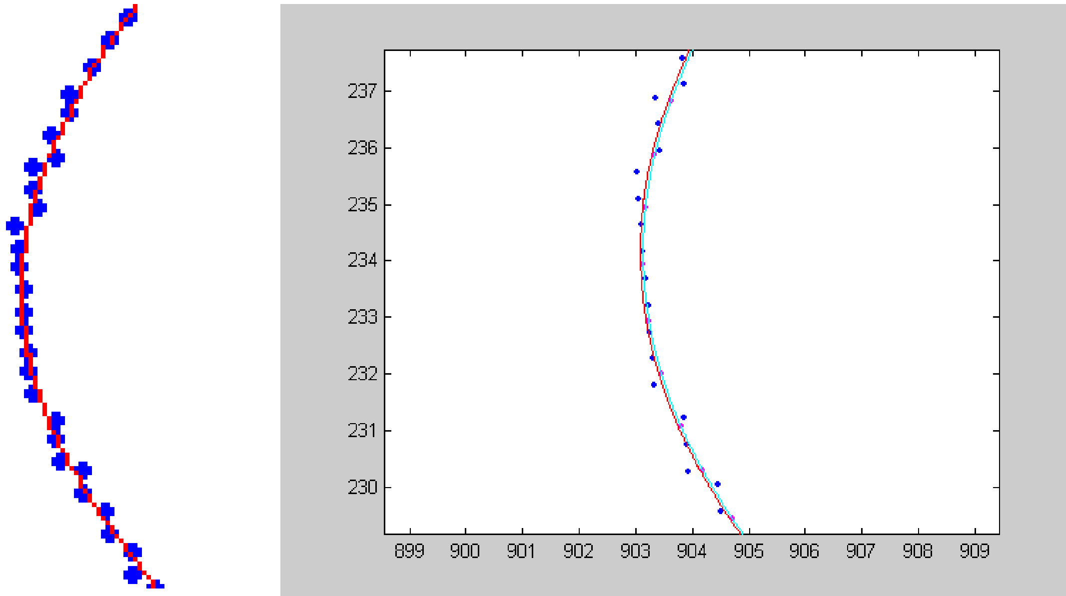


(a) (b)

**Figure 5.** Curve fitting:
(a) LiDAR points (blue) and fitted curve (red)
(b) LiDAR data and GPS-surveyed points (magenta) and fitted curve (cyan).

## Curve Matching

The objective of curve matching is to find the spatial relationship between two data representations of the pavement markings. Because there is no point-to-point correspondence between the two data sets, point-based transformations are directly not applicable. Furthermore, the somewhat modest horizontal accuracy of the LiDAR points is an additional disadvantage. Using linear features, however, presents a solution that is less sensitive compared to point-based methods. Assuming that the two representations, such as the curve fitted ones, provide an adequate description of the same shape, the problem is simply how to match two free-shape curves. The pavement markings descriptions in both original and curve-fitted format are spatially close to each other, the well-known Iterative Closest Point (ICP) algorithm (Besl and McKay, 1992; Madhavan et al., 2005) was selected to perform that task.

Iterative registration algorithms are increasingly used for registering 2D/3D curves and range images recently. The ICP algorithm is adopted here to match curves describing pavement markings obtained from LiDAR intensity and GPS measurements. The ICP algorithm finds the best correspondence between two curves (point sets) by iteratively determining the translations and rotations parameters of a 2D/3D rigid body transformation.

$$\min_{(R,T)} \sum_i \left\| M_i - (RD_i + T) \right\|^2$$

where $R$ is a 3*3 rotation matrix, $T$ is a 3*1 translation vector and subscript $i$ refer to the corresponding points of the sets M (model) and D (data). The ICP algorithm can be summarized as follows:

1. For each point in D, compute the closest point in M
2. Compute the incremental transformation ($R$, $T$)
3. Apply incremental transformation from step (2) to D
4. If relative changes in $R$ and $T$ are less than a given threshold, terminate, otherwise go to step (1)

ICP can be applied to individual pavement markings or to a group of pavement markings. Figure 6 shows an intersection where four lines were matched.

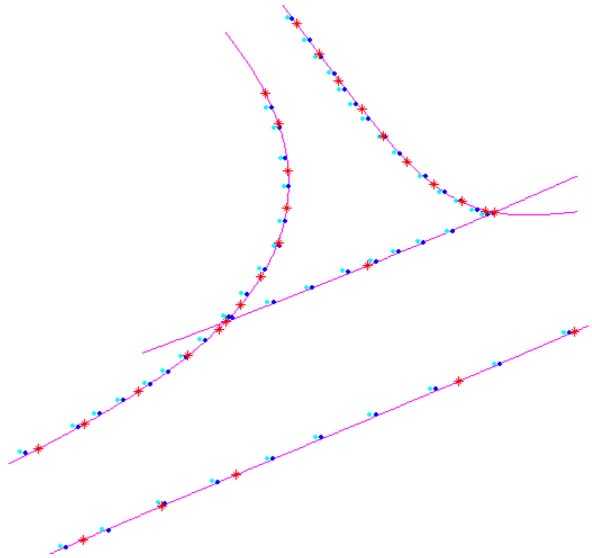

**Figure 6.** Curve matching based on four curves; magenta: curves fitted to control points, red: GPS control points, blue: transformed curve points after ICP, and cyan: curve points derived from LiDAR.

## EXPERIMENTAL RESULTS

To support performance testing of the proposed method, the Ohio Department of Transportation surveyed several intersections in an area which was recently LiDAR surveyed. The pavement markings were surveyed using a VRS system with about 1-2 cm horizontal and 2-5 cm vertical accuracy; the point spacing varied in the 1-3 pts/m range. Figure 7 shows an area with linear pavement markings measured from the LiDAR intensity data as well as the GPS points; for better illustration only the operator-measured LiDAR points, which were considered as reference, are shown. Note the small yet clearly visible misfit between the two point sets.

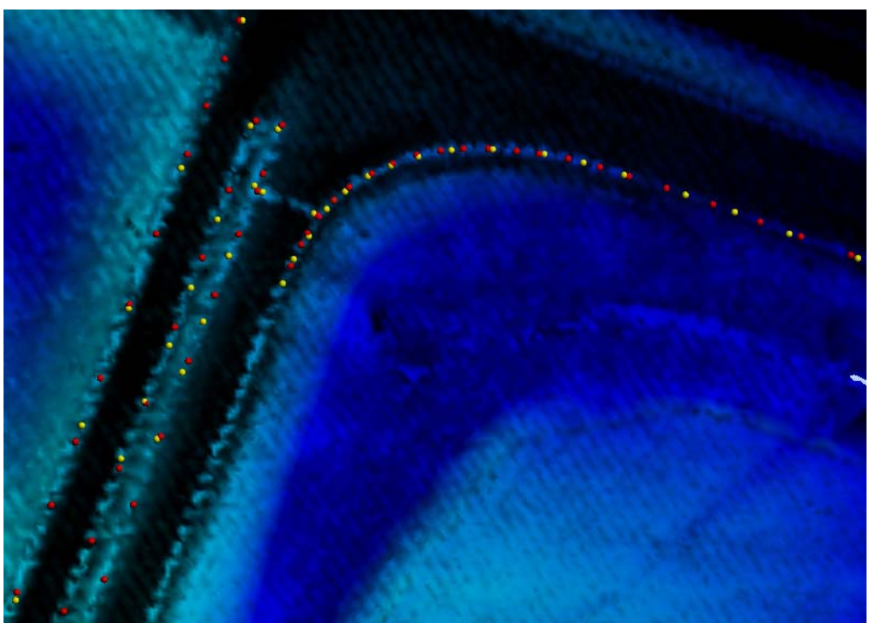

**Figure 7**. Intersection with pavements markings measured from LiDAR intensity data (points marked yellow) and GPS-surveyed points (red).

In the curve fitting process both data representations were fitted, with a point spacing of 1 cm, and various combinations were processed by ICP-based curve matching in 2D and 3D. In order to assess the accuracy of the transformation, the correspondence between the LiDAR-derived curve and the control curve were established. Since the two curves in general are not totally identical, even after the final ICP iteration, the transformed LiDAR-derived points are close but not necessarily fall on the control curve. However, the location of the transformed LiDAR-derived points represents the best fit to the control curve in least squares sense. Therefore, these points are projected to the closest points of the control curve, and then they are considered as conjugate points. The transformation parameters between these two point sets (the original LiDAR-derived points and their corresponding points on the control curve) are calculated in a least squares adjustment. In this computation, the 2D transformation parameters for a representative test data set were estimated at $\sigma_{\Delta X} = \pm\ 0.013$m, $\sigma_{\Delta Y} = \pm\ 0.010$m, and $\sigma_{angle} = \pm\ 1.95$ arcmin, indicating that a good match was found with the ICP method. The numerical values, including the transformation parameters and error terms, are listed in Tables I and II.

**Table 1**. Transformation results (2D).

| **Transformation parameter** | **ICP-adjusted results [m, °]** | **Estimated accuracy [m, °]** |
|---|---|---|
| ΔX | 0.041 | 0.013 |
| ΔY | -0.023 | 0.010 |
| φ | -0.000 | 0.03 |

The ~2 cm horizontal accuracy could be considered excellent given the fact that the GPS-surveyed points are known, at best, 1 cm-level accuracy and the LiDAR-based pavement marking positioning accuracy is estimated at the few cm range.

Since the overall LiDAR data quality used for testing was quite good, the discrepancies found at several intersections were rather small, a simulated error was introduced to test the method for less than ideal situations. Using the same data set, a 16 and -4 cm horizontal offset was added to the X and Y coordinates of the LiDAR point measurements, respectively. Tables II and III show the residuals measured at the pavement markings before and after the correction.

**Table 2.** Initial residuals.

| | **ΔX [m]** | **ΔY [m]** |
|---|---|---|
| Mean | 0.158 | -0.036 |
| STD | 0.048 | 0.045 |

**Table 3**. Residuals after correction.

| | **ΔX [m]** | **ΔY [m]** |
|---|---|---|
| Mean | 0.000 | -0.000 |
| STD | 0.048 | 0.045 |

## CONCLUSION

The introduced method to use pavement markings as ground control showed good initial performance. Using a data set acquired by a state-of-the-art LiDAR system, the performance of the three main processing steps was validated. In all the cases, the curve fitting and ICP-based matching delivered robust results. The extraction of pavement markings, however, has experienced difficulties in some cases where the intensity data were noisier. A key advantage of using pavement markings is that they can be quickly surveyed with GPS VRS technique.

## ACKNOWLEDGEMENTS

The authors would like to thank the Ohio Department of Transportation for the GPS survey of pavement markings and flying LiDAR surveys to acquire essential data for this research.

## REFERENCES

ASPRS LiDAR Committee, 2004. ASPRS Guidelines Vertical Accuracy Reporting for LiDAR Data, http://www.asprs.org/society/committees/lidar/Downloads/Vertical_Accuracy_Reporting_for_Lidar_Data.pdf.

Besl, P. J. and McKay, N. D., 1992. A method for registration of 3-d shapes, *IEEE Trans. Pat. Anal. and Mach. Intel.* 14(2), pp 239-256, Feb 1992.

Burman, H., 2002. Laser strip adjustment for data calibration and verification, *International Archives of Photogrammetry and Remote Sensing*, 34 (Part 3A): 67-72.

Csanyi N, Toth C., Grejner-Brzezinska D. and Ray J., 2005. Improving LiDAR data accuracy using LiDAR-specific ground targets, In *Proceedings of the ASPRS 2005 Annual Conference*, Baltimore, MD, March 7-11, CD-ROM.

Csanyi, N. and Toth, C., 2007. Improvement of LiDAR data accuracy using LiDAR-specific ground targets, *Photogrammetric Engineering & Remote Sensing*, Vol. 73, No. 4, pp. 385-396.

Gruen, A., Akca, D., 2005. Least squares 3D surface and curve matching, *ISPRS Journal of Photogrammetry and Remote Sensing*, 59 (3), 151-174.

Hasegawa, H., 2006. Evaluations of LiDAR reflectance amplitude sensitivity towards land cover conditions, *Bulletin of the Geographical Survey Institute*, Vol. 53.

Ichida, K. and Kiyono, T.1977. Curve fitting with one-pass method with a piecewise cubic polynomial, *ACM Transactions on Mathematical Software*, Vol. 3, No. 2, pp. 164-174.

Kager, H. and Kraus, K., 2001. Height discrepancies between overlapping laser scanner strips, In *Proceedings of Optical 3D Measurement Techniques V*, Vienna, Austria: 103-110.

Maas, H.-G., 2001. On the use of pulse reflectance data for laserscanner strip adjustment, *International Archives of Photogrammetry, Remote Sensing and Spatial Information Sciences*, 33 (Part 3/W4): 53-56.

Madhavan, R., Hong, T., Messina, E., 2005. Temporal range registration for unmanned ground and aerial vehicles, *Journal of Intelligent and Robotic Systems*, Volume 44, Number 1 / September, 2005, pp. 47-69.

Toth, C., D. Brzezinska, N. Csanyi, E. Paska and N. Yastikly, 2007a. LiDAR mapping supporting earthquake research of the San Andreas fault, In *Proceedings of the ASPRS 2007 Annual Conference*, Tampa, Florida, May 7–11, CD ROM.

Toth, C., Paska, E., Grejner-Brzezinska, D.A., 2007b. Using pavement markings to dupport the QA/QC of LiDAR fata, Photogrammetric Image Analysis (PIA 2007), *International Archives of Photogrammetry and Remote Sensing*, Vol. XXXVI, 3/W49B, pp. 173-178.